Lecture 3

SPECIFICATION FOR CARBON STEEL ELECTRODES AND FLUXES FOR SUBMERGED ARC WELDING

SFA-5.17

(Identical with AWS Specification A5.17-89)

1. Scope

This specification prescribes requirements for the classification of carbon steel electrodes (both solid and composite) and fluxes for submerged arc welding.

SECTION A — GENERAL REQUIREMENT

2. Classification

2.1 The welding electrodes and fluxes covered by the specification are classified according to the following:

(a) The mechanical properties of the weld metal obtained with a combination of a particular flux and a particular classification of electrode, as specified in Tables 5 and 6;

(b) The condition of heat treatment in which those properties are obtained, as specified in para. 8.4 (and shown in Fig. 1)

(c) The chemical composition of the electrode (for solid electrodes) as specified in Table 1, or the weld metal produced with a particular flux (for composite electrodes) as specified in Table 2.

2.2 Electrodes classified under one classification shall not be classified under any other classification in this specification, except that solid electrodes meeting the chemical composition requirements of both the EL8 and EL12 classification (Table 1) may be given both classifications. Fluxes may be classified under any number of classifications, for weld metal in either or both the as-welded and postweld heat treated conditions, or using different electrode classifications. The classification system is shown in Fig. 1.

2.3 The electrodes and fluxes classified under this specification are intended for submerged arc welding, but that is not to prohibit their use with any other process for which they are found suitable.

3. Acceptance

Acceptance of the materials shall be in accordance with the provisions of the latest edition of AWS A5.01, *Filler Metal Procurement Guidelines*[1] (see Appendix A3).

4. Certification

By affixing the AWS Specification and Classification designations to the packaging, the manufacturer certifies that the product meets the requirements of this specification (see Appendix A4).

5. Units of Measure and Rounding-Off Procedure

5.1 U.S. Customary Units are the standard units of measure in this specification. The SI Units are given as equivalent values to the U.S. Customary Units. The standard sizes and dimensions in the two systems are not identical, and, for this reason, conversion from a standard size or dimension in one systems will not always coincide with a standard size or dimension in the other. Suitable conversions encompassing standard sizes of both can be made, however, if appropriate tolerances are applied in each case.

5.2 For the purpose of determining conformance with this specification, an observed or calculated value shall be rounded to the nearest 1000 psi for tensile

[1] AWS standards may be obtained from the American Welding Society, 550 N.W. LeJeune Road, P.O. Box 351040, Miami, Florida 33135.

TABLE 1
CHEMICAL COMPOSITION REQUIREMENTS FOR SOLID ELECTRODES

Electrode Classification	UNS Number[3]	wt. percent[1] [2]					
		C	Mn	Si	S	P	Cu[4]
Low Manganese Electrodes							
EL8	K01008	0.10	0.25/0.60	0.07	0.030	0.030	0.35
EL8K	K01009	0.10	0.25/0.60	0.10/0.25	0.030	0.030	0.35
EL12	K01012	0.04/0.14	0.25/0.60	0.10	0.030	0.030	0.35
Medium Manganese Electrodes							
EM12	K01112	0.06/0.15	0.80/1.25	0.10	0.030	0.030	0.35
EM12K	K01113	0.05/0.15	0.80/1.25	0.10/0.35	0.030	0.030	0.35
EM13K	K01313	0.06/0.16	0.90/1.40	0.35/0.75	0.030	0.030	0.35
EM14K	K01314	0.06/0.19	0.90/1.40 (Ti 0.03/0.17)	0.35/0.75	0.025	0.025	0.35
EM15K	K01515	0.10/0.20	0.80/1.25	0.10/0.35	0.030	0.030	0.35
High Manganese Electrodes							
EH11K	K11140	0.07/0.15	1.40/1.85	0.80/1.15	0.030	0.030	0.35
EH12K	K01213	0.06/0.15	1.50/2.00	0.25/0.65	0.025	0.025	0.35
EH14	K11585	0.10/0.20	1.70/2.20	0.10	0.030	0.030	0.35

NOTES:
(1) The filler metal shall be analyzed for the specific elements for which values are shown in this table. If the presence of other elements is indicated, in the course of this work, the amount of those elements shall be determined to ensure that their total (excluding iron) does not exceed 0.50 percent.
(2) Single values are maximum.
(3) SAE/ASTM Unified Numbering System for Metals and Alloys.
(4) The copper limit includes any copper coating that may be applied to the electrode.

7. Retest

If any test fails to meet its requirement, that test shall be repeated twice. The results of both tests shall meet the requirement. Samples for retest may be taken from the original test assembly or from one or two new test assemblies. For chemical analysis, retest need be only for those specific elements that failed to meet their requirement.

TABLE 2
CHEMICAL COMPOSITION REQUIREMENTS FOR COMPOSITE ELECTRODE WELD METAL

Electrode Classification	wt. percent[1] [2] [3]					
	C	Mn	Si	S	P	Cu
EC1	0.15	1.80	0.90	0.035	0.035	0.35

NOTES:
(1) The weld metal shall be analyzed for the specific elements for which values are shown in this table. If the presence of other elements is indicated, in the course of this work, the amount of those elements shall be determined to ensure that their total (excluding iron) does not exceed 0.50 percent.
(2) Single values are maximum.
(3) A low dilution area of the groove weld of Fig. 3 or the fractured tension test specimen of Fig. 5 may be substituted for the weld pad, and shall meet the above requirements. In case of dispute, the weld pad shall be the referee method.

8. Weld Test Assemblies

8.1 No weld test assemblies are required for classification of solid electrodes. One weld test assembly is required for classification of composite electrodes. It is the weld pad in Fig. 2 for chemical analysis of the low dilution weld metal.

In addition to the above, one weld test assembly is required for each classification of an electrode-flux combination. This is the groove weld in Fig. 3 for mechanical properties and soundness of the weld metal. Note (3) to Table 2 allows the sample for chemical analysis in the case of a composite electrode to be taken from a low dilution area in the groove weld, Fig. 3, or from the fractured tension test specimen, Fig. 5, thereby avoiding the need to make the weld pad. In case of dispute, the weld pad shall be the referee method. When a Certificate of Test is prepared, it shall indicate wheth-

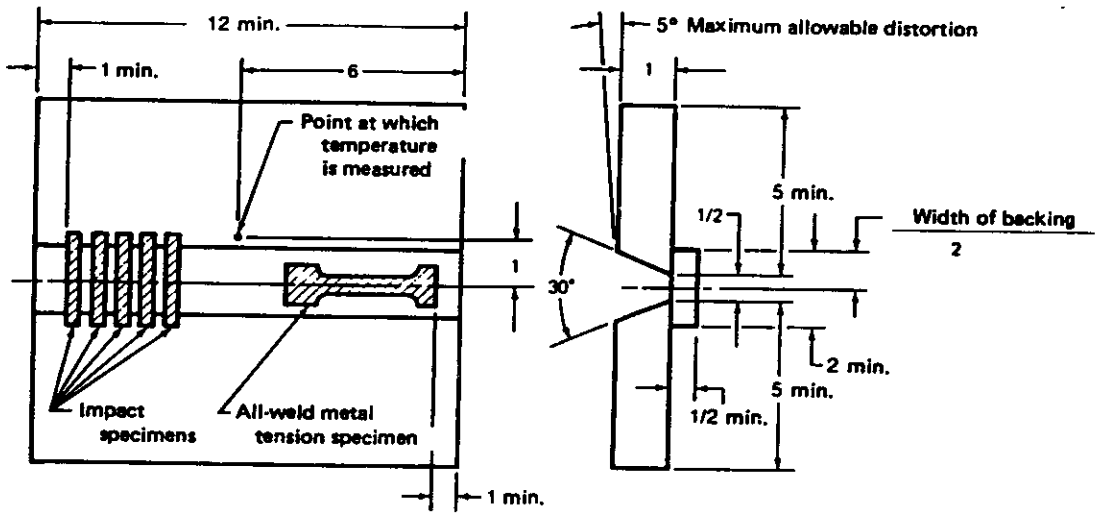

(A) Joint Configuration and Location of Test Specimens

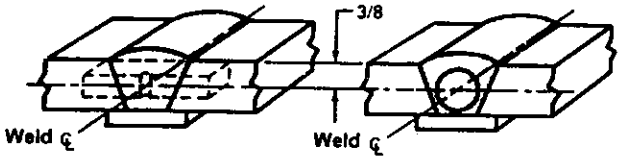

(B) Location of Impact Test Specimens

(c) Location of Tension Test Specimen

Note: All dimensions except angles are in inches.

SI EQUIVALENTS

in.	mm
1/16	1.6
1/4	6.4
3/8	9.5
1/2	13
3/4	19
1	25
5	127
6	152
12	305

Welding Conditions for Solid Electrodes [a,b]

Electrode Size[c] in.	Electrode Size[c] mm	Amperage[d] (± 25)	Voltage[e] (± 1)	Welding Current	Travel Speed ipm (± 1)	Travel Speed mm/s (± 0.4)	Base[f] Metal	Preheat Temperature[g]	Interpass Temperature[g]
1/16	1.6	350	28	D.C. either polarity	12	5.1	ASTM A36, A285 Grade C, A515 Grade 70, or A516 Grade 70	65 to 325°F (18 to 163°C)	275 to 325°F (135 to 163°C)
5/64	2.0	400	28		13	5.5			
3/32	2.4	450	28		14	5.9			
1/8	3.2	500	28		15	6.3			
5/32	4.0	550	28		16	6.8			
3/16	4.8	600	28		17	7.2			
7/32	5.6	650	28		18	7.6			
1/4	6.4	Not Specified	Not Specified		Not Specified[h]				

a. The first layer shall be produced in either 1 or 2 passes. All other layers shall be produced in 2 or 3 passes per layer except the last, which shall be produced in 3 or 4 passes. These welding conditions are intended for machine or automatic welding.
b. Welding conditions for composite electrodes shall be as agreed between purchaser and supplier.
c. Classification is based on the properties of weld metal with 5/32 in. (4.0 mm) electrodes or the closest size manufactured, if 5/32 in. (4.0 mm) is not manufactured. The conditions given above for sizes other than 5/32 in. (4.0 mm) are to be used when classification is based on those sizes, or when they are required for lot acceptance testing under A5.01, *Filler Metal Procurement Guidelines* (unless other conditions are specified by the purchaser).
d. Lower amperages may be used for the first layer.
e. Contact tube-to-work distance is 1/2 to 3/4 in. (13 to 19 mm) for 1/16 and 5/64 in. (1.6 and 2.0 mm) electrodes; 3/4 to 1¼ in. (19 to 32 mm) for 3/32 in. (2.4 mm) electrodes; and 1 to 1½ in. (25 to 38 mm) for 1/8, 5/32, 3/16, and 7/32 in. (3.2, 4.0, 4.8 and 5.6 mm) electrodes. When an electrode manufacturer recommends a contact tube-to-work distance outside the range shown, those recommendations shall be followed within 1/4 in. (6 mm).
f. In case of dispute, A36 steel and DCEP (electrode positive) shall be used as the referee base metal and current.
g. The first bead shall be produced with the assembly at any temperature between 65 and 325°F (18 to 136°C). Welding shall continue, bead by bead, until a temperature within the interpass temperature range has been attained. Thereafter, production of subsequent beads may begin only when the assembly is within the interpass temperature range.
h. When a test assembly is required for 1/4 in. (6.4 mm) electrodes, the welding conditions shall be as agreed between purchaser and supplier.

FIG. 3 GROOVE WELD TEST ASSEMBLY

metal. Both surfaces of the test assembly, in the area of the weld, shall be smooth enough to avoid difficulty in interpreting the radiograph.

10.2 The weld shall be radiographed in accordance with ASTM method E 142 *Controlling Quality of Radiographic Testing.* The quality level of inspection shall be 2-2T.

10.3 The soundness of the weld metal meets the requirements of this specification if the radiograph does not show:

(a) Cracks, incomplete fusion, or incomplete penetration;

(b) Slag inclusions longer than ¼ in. (6 mm) or ⅓ of the thickness of the weld, whichever is greater, or groups of slag inclusions in line that have an aggregate length greater than the thickness of the weld in a length 12 times the thickness of the weld except when the distance between the successive inclusions exceeds six times the length of the longest inclusion in the group.

(c) Rounded indications in excess of those permitted by the radiographic standards in Fig. 4.

One inch of the weld, measured from each end of the test assembly, shall be disregarded from radiographic evaluation.

11. Tension Test

11.1 One all-weld-metal tension test specimen shall be machined from the groove weld described in para. 8.4 and shown in Fig. 3. The dimensions of the specimen shall be as shown in Fig. 5.

11.2 The specimen shall be tested in the manner described in the tension test section of the latest edition of ANSI/AWS B4.0, *Standard Methods for Mechanical Testing of Welds.*

11.3 The results of the tension test shall meet the requirements specified in Table 5.

12. Impact Test

12.1 Five Charpy V-notch impact specimens (Fig. 6) shall be machined from the test assembly shown in Fig. 3 for those classifications for which impact testing is required in Table 6.

12.2 The five specimens shall be tested in accordance with the impact test section of ANSI/AWS B4.0. The test temperature shall be that specified in Table 6 for the classification under test.

12.3 In evaluating the test results, the lowest and the highest values obtained shall be disregarded. Two of the remaining three values shall equal, or exceed, the specified 20 ft-lb (27 J) energy level. One of the three may be lower, but not lower than 15 ft-lbs (20 J), and the average of the three shall not be less than the required 20 ft-lb (27 J) energy level.

SECTION C — MANUFACTURE, IDENTIFICATION AND PACKAGING

13. Method of Manufacture

The electrodes and flues classified according to this specification may be manufactured by any method that will produce material that meets the requirements of this specification.

14. Electrode Requirements

14.1 Standard Sizes. Standard sizes for electrodes in the different package forms (coils with support, coils without support, and drums) are shown in Table 7.

14.2 Finish and Uniformity

14.2.1 The electrode shall have a smooth finish which is free from slivers, depressions, scratches, scale, seams and laps (exclusive of the longitudinal joint in composite electrodes), and foreign matter that would adversely affect the welding characteristics, the operation of the welding equipment, or the properties of the weld metal.

14.2.2 A Each continuous length of electrode shall be from a single heat or lot of material, and welds, when present, shall have been made so as not to interfere with the uniform, uninterrupted feeding of the electrode on automatic and semiautomatic equipment.

14.2.3 Core ingredients in composite electrodes shall be distributed with sufficient uniformity throughout the length of the electrode so as not to adversely affect the performance of the electrode or the properties of the weld metal.

14.2.4 A suitable protective coating, such as copper, may be applied to any electrode covered in this specification.

14.3 Standard Package Forms

14.3.1 Standard package forms are coils with support, coils without support, and drums. Standard package dimensions and weights for each form are given in Table 8. Package forms, sizes and weights other than these shall be as agreed between purchaser and supplier.

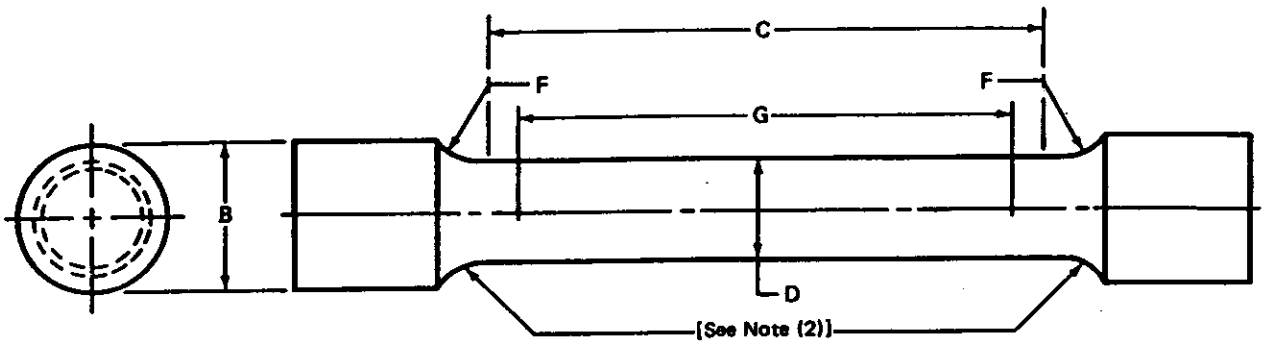

Dimensions of Specimen, in.						
Test Plate Thickness	D	G	C	B	F, MIN	Approximate Area, in.²
1	0.500 ±0.010	2.000 ± 0.005	2–1/4	3/4	0.375 (3/8)	1/5

Dimensions of Specimen, mm						
Test Plate Thickness	D	G	C	B	F, MIN	Approximate Area, mm²
25.4	12.7 ± 0.25	50.8 ± 0.13	57.1	19.1	9.5	129

NOTES:
(1) Dimensions G and C shall be as shown, but the ends may be as required to fit the testing machine holders as long as the load is axial.
(2) The diameter of the specimen within the gage length shall be slightly smaller at the center than at the ends. The difference shall not exceed one percent of the diameter.
(3) The finish of the surface within the C dimension shall be no rougher than 63 μ in. (1.6 μ m).

FIG. 5 DIMENSIONS OF TENSION TEST SPECIMEN

TABLE 5
TENSION TEST REQUIREMENTS

Flux Classification[1]	Tensile Strength		Yield Strength min.[2]		Elongation % min.[2]
	psi	MPa	psi	MPa	
F6XX-EXXX	60 000/80 000	415/550	48 000	330	22
F7XX-EXXX	70 000/95 000	480/650	58 000	400	22

NOTES:
(1) The letter "X" used in various places in the classifications in this table stands for, respectively, the condition of heat treatment, the toughness of the weld metal, and the classification of the electrode (see Fig. 1).
(2) Yield strength at 0.2 percent offset and elongation in 2 in. (51 mm) gage length.

TABLE 7
STANDARD ELECTRODE SIZES AND TOLERANCES[1]

Size (Diameter)		Tolerance			
		Solid (E)		Composite (EC)	
in.	mm	±in.	±mm	±in.	±mm
1/16 (0.0625)	1.6	0.002	0.05	0.005	0.13
5/64 (0.078)	2.0	0.002	0.05	0.006	0.15
3/32 (0.094)	2.4	0.002	0.05	0.006	0.15
1/8 (0.125)	3.2	0.003	0.08	0.007	0.18
5/32 (0.156)	4.0	0.004	0.10	0.008	0.20
3/16 (0.188)	4.8	0.004	0.10	0.008	0.20
7/32 (0.219)	5.6	0.004	0.10	0.008	0.20
1/4 (0.250)	6.4	0.004	0.10	0.008	0.20

NOTE:
(1) Other sizes and tolerances may be supplied as agreed between purchaser and supplier.

aged to ensure against damage during shipment and storage under normal conditions.

14.7 Marking of Packages

14.7.1 The following product information (as a minimum) shall be legibly marked so as to be visible from the outside of each unit package.

(a) AWS specification and classification number (year of issue may be excluded);

(b) Supplier's name and trade designation;

(c) In the case of a composite electrode, the trade designation of the flux (or fluxes) with which its weld metal composition meets the requirements of Table 2;

(d) Size and net weight;

TABLE 8
STANDARD DIMENSIONS AND WEIGHTS[1]

Electrode Size[2]		Net[3] Weight of Coil		Inside Diameter of Liner		Width of Coil, Max.		Outside Diameter of Coil, Max.	
in.	mm	lb	kg	in.	mm	in.	mm	in.	mm
Coils With Support									
1/16–1/4	1.6–6.4	25	11	12 ± 1/8	305 ± 3	2 1/2	65	17 1/2	445
		50	23			4 3/4	120	17	430
		60	27						
		65	30						
5/32–1/4	2.4–6.4	100	45	(4)		5	125	31 1/2	800
		150	68						
		200	91						
Coils Without Support									
1/16–1/4	1.6–6.4	— — — As agreed between purchaser and supplier — — —							
Drums									
1/16–1/4	1.6–6.4	— — — As agreed between purchaser and supplier — — —						20[5]	500[5]
								23[5]	600[5]

NOTES:
(1) Other dimensions and weights may be supplied as agreed between purchaser and supplier.
(2) The range is inclusive.
(3) Net weights shall not vary more than ± 10 percent.
(4) The diameter of the liner shall be as agreed between purchaser and supplier.
(5) Outside diameter of drums is nominal, not maximum.

- Wear correct eye, ear and body protection.
- Do not touch live electrical parts.
- See American National Standard Z49.1, *Safety in Welding and Cutting*, published by the American Welding Society, 550 N.W. LeJeune Road, P.O. Box 351040, Miami, Florida 33135; OSHA Safety and Health Standards, 29 CFR 1910, available from the U.S. Government Printing Office, Washington, DC 20402

DO NOT REMOVE THIS LABEL

Appendix
Guide to ANSI/AWS A5.17-89, Specification for Carbon Steel Electrodes and Fluxes for Submerged Arc Welding

(This Appendix is not a part of ANSI/AWS A5.17-89, *Specification for Carbon Steel Electrodes and Fluxes for Submerged Arc Welding*, but is included for information purposes only.)

A1. Introduction

The purpose of this guide is to correlate the electrode and flux classification with their intended applications so the specification can be used effectively. Reference to appropriate base metal specifications is made whenever that can be done and when it would be helpful. Such references are intended only as examples rather than complete listings of the base metals for which each electrode and flux combination is suitable.

A2. Classification System

A2.1 Classification of Electrodes. The system for identifying the electrode classifications in this specifications follows the standard pattern used in other AWS filler metal specifications. The letter "E" at the beginning of each classification designation stands for electrode. The remainder of the designation indicates the chemical composition of the electrode, or, in the case of composite electrodes, of the low dilution weld metal obtained with a particular flux. See Fig. 1.

The letter "L" indicates that the solid electrode is comparatively low in manganese content. The letter "M" indicates a medium manganese content, while the letter "H" indicates a comparatively high manganese content. The one or two digits following the manganese designator indicate the nominal carbon content of the electrode. The letter "K", which appears in some designations, indicates that the electrode is made from a heat of silicon-killer steel. Solid electrodes are classified only on the basis of their chemical composition, as specified in Table 1 of this specification.

A composite electrode is indicated by the letter "C" after the "E", and a numerical suffix. The composition of a composite electrode is meaningless and the user is therefore referred to weld metal composition (Table 2) with a particular flux, rather than to electrode composition.

A2.2 Classification of Fluxes. Fluxes are classified on the basis of the mechanical properties of the weld metal they produce with some certain classification of electrode, under the specific test conditions called for in Section B of this specification.

As examples of flux classifications, consider the following:

F6A0-EH14
F7P6-EM12K
F7P4-EC1

The prefix "F" designates a flux. This is followed by a single digit representing the minimum tensile strength required of the weld metal in 10 000 psi increments.

When the letter "A" follows the strength designator, it indicates that the weld metal was tested (and is classified) in the as-welded condition. When the letter "P" follows the strength designator, it indicates that the weld metal was tested (and is classified) after postweld heat treatment called for in the specification. The digit that follows the A or P will be a number or the letter "Z". This digit refers to the impact strength of the weld metal. Specifically, it designates the temperature at (and above) which the weld metal meets, or exceeds, the required 20 ft-lb (27 J) Charpy V-notch impact strength (except for the letter Z, which indicates that no impact requirement is specified — see Table 6). These mechanical property designations are followed

weld metal chemical analysis as a result of a large change in the arc voltage, and thus, the arc length.

The primary use for neutral fluxes is in multiple pass welding, especially when the base metal exceeds 1 in. (25 mm) in thickness.

Note the following considerations concerning neutral fluxes:

(a) Since neutral fluxes contain little or no deoxidizers, they must rely on the electrode to provide deoxidation. Single pass welds with insufficient deoxidation on heavily oxidized base metal may be prone to porosity, centerline cracking, or both.

(b) While neutral fluxes do maintain the chemical composition of the weld metal even when the voltage is change, it is not always true that the chemical composition of the weld metal is the same as the chemical composition of the electrode used. Some neutral fluxes decompose in the heat of the arc and release oxygen, resulting in a lower carbon value in the weld metal than the carbon content of the electrode itself. Some neutral fluxes contain manganese silicate which can decompose in the heat of the arc to add some manganese and silicon to the weld metal even though no metallic manganese or silicon was added to these particular fluxes. These changes in the chemical composition of the weld metal are fairly consistent even when there are large changes in voltage.

(c) Even when a neutral flux is used to maintain the weld metal chemical composition through a range of welding voltages, weld properties such as strength level and impact properties can change because of changes in other welding parameters such as depth of fusion, heat input, and number of passes.

A6.1.2 Active Fluxes. Active fluxes are those which contain small amounts of manganese, silicon, or both. These deoxidizers are added to the flux to provide improved resistance to porosity and weld cracking caused by contaminants on or in the base metal.

The primary use for active fluxes is to make single pass welds, especially on oxidized base metal.

Note the following considerations concerning active fluxes:

(a) Since active fluxes do contain some deoxidizers, the manganese, silicon, or both in the weld metal will vary with changes in arc voltage. An increase in manganese or silicon increases the strength of the weld metal in multiple pass welds but may lower the impact properties. For this reason, voltage must be more tightly controlled for multiple pass welding with active fluxes than when using neutral fluxes.

(b) Some fluxes are more active than others. This means they offer more resistance to porosity due to base metal surface oxides in single pass welds than a flux which is less active, but may pose more problems in multipass welding.

A6.1.3 Alloy Fluxes. Alloy fluxes are those which can be used with a carbon steel electrode to make alloy weld metal. The alloys for the weld metal are added as ingredients in the flux.

The primary use for alloy fluxes is to weld low alloy steels and for hardfacing. As such, they are outside of the scope of this specification. See the latest edition of ANSI/AWS A5.23, *Specification for Low Alloy Steel Electrodes and Fluxes for Submerged Arc Welding,* for a more complete discussion of alloy fluxes.

A6.1.4 Wall Neutrality Number. The Wall Neutrality Number is a convenient relative measure of flux neutrality. The Wall Neutrality Number addresses fluxes and electrodes for welding carbon steel with regard to the weld metal manganese and silicon content. It does not address alloy fluxes. For an electrode-flux combination to be considered neutral, it should have a Wall Neutrality Number of 40 or less. The lower the wall neutrality number, the more neutral is the flux.

Determination of the Wall Neutrality Number (N) can be done in accordance with the following:

(a) A weld pad of the type required in the specification is welded with the electrode-flux combination being tested. Welding parameters are the same as those specified for the weld test plate for the diamter electrode being used.

(b) A second weld pad is welded using the same parameters, except that the arc voltage is increased by 8 volts.

(c) The top surface of each of the weld pads is ground or machined smooth to clean metal. Samples sufficient for analysis are removed by machining. Weld metal is analyzed only from the top (fourth) layer of the weld pad. The samples are analyzed separately for silicon and manganese.

(d) The Wall Neutrality Number depends on the change in silicon, regardless of whether it increases or decreases, and on the change in manganese, regardless of whether it increase or decreases. The Wall Neutrality Number is the absolute value (ignoring positive or negative signs) and is calculated as follows:

$$N = 100\ (|\Delta\%Si| + |\Delta\%Mn|)$$

where:

$\Delta\%Si$ = is the difference in silicon levels of the two pads and

$\Delta\%Mn$ = is the corresponding difference in manganese levels.

tions of those beads. For this reason, the properties of a single-pass weld may be somewhat different from those of a multipass weld made with the same electrode and flux.

The weld metal properties in this specification are determined either in the as-welded condition or after a postweld heat treatment (one hour at 1150°F [621°C]), or both. Most of the weld metals are suitable for service in either condition, but the specification cannot cover all of the conditions that such weld metals may encounter in fabrication and service. For this reason, the classifications in this specification require that the weld metals be produced and tested under certain specific conditions encountered in practice. Procedures employed in practice may require voltage, amperage, type of current, and travel speeds that are considerably different from those required in this specification. In addition, differences encountered in electrode size, electrode extension, joint configuration, preheat, interpass temperatures, and postweld heat treatment can have a significant effect on the properties of the joint. Extended postweld heat treatment (conventionally 20 to 30 hours for extremely thick sections) may have a major influence on the strength and toughness of the weld metal. Both can be substantially reduced. The user needs to be aware of this and of the fact that the mechanical properties of carbon steel weld metal produced with other procedures may differ from the properties required by Tables 5 and 6 of this specification.

A6.4 Diffusible Hydrogen. Submerged arc welding is normally a low hydrogen welding process when care is taken to maintain the flux in a dry condition. In submerged arc welding with carbon steel electrodes and fluxes classified in the specification, weld metal or heat-affected zone cracking associated with diffusible hydrogen is generally not a problem. Exceptions may arise when joining high carbon steels or when using carbon steel electrodes to weld on low alloy high strength steels (e.g., for a joint of carbon steel to low alloy steel).

If an assessment of the diffusible hydrogen content is to be made. The method of ANSI/AWS A4.3-86, *Standard Procedures for Determination of the Diffusible Hydrogen Content of Martensitic, Bainitic, and Ferritic Steel Weld Metal Produced by Arc Welding,* is appropriate.

Effect of Electrochemical Reactions on Submerged Arc Weld Metal Compositions

Weld metal composition is controlled by chemical reactions in four separate areas during welding

BY J. H. KIM, R. H. FROST, D. L. OLSON AND M. BLANDER

ABSTRACT. The purpose of this work is to investigate the relative influence of electrochemical and thermochemical reactions on the weld metal chemistry in a direct current submerged arc welding process. Chemical analyses were carried out on the melted electrode tips, the detached droplets and the weld metal for both electrode-positive (reverse) polarity where the welding wire is anodic and electrode-negative (straight) polarity where the welding wire is cathodic. The results suggest that both thermochemical and electrochemical reactions are important in altering the composition of the weld metal. The anodic electrochemical reactions include the oxidation of iron and alloy elements, and the discharge and pickup of oxygen anions from the molten flux. Cathodic electrochemical reactions include the reduction of iron and alloy elements from the flux to the metal phase, and the refining of oxygen. Thermochemical reactions occur and move the overall composition toward the thermochemical equilibrium.

Introduction

The submerged arc welding process uses a protective flux cover with a consumable welding wire. The welding current is carried largely by the submerged arc and to some extent by conduction in the molten flux layer. Information on the interaction between slag and weld metal is significant for a better understanding of the arc welding process. Although slag/metal reactions are of importance in many fusion welding processes and are often referred to in the literature, comparatively little is known about the mechanisms that control them.

The chemistry in steel making tends to be dominated by thermochemical reactions because they generally involve large surface areas, low current densities and alternating current power. But a direct current submerged arc welding process involves small surface areas and high current densities. Therefore, it is expected that electrochemical reactions, as well as thermochemical reactions, will exert a significant influence over the final chemistry of the weld.

The overall composition of the weld is controlled by the composition of the metal droplets that enter the weld pool and by the amount of dilution of the weld pool by the base plate. These compositions are controlled by chemical reactions at four separate zones: the melted electrode tip, the detached droplet, the hot weld pool immediately below the arc, and the cooling and solidifying weld pool behind the arc. Thermochemical reactions occur at all four zones and move the chemistry in the direction of chemical equilibrium. But electrochemical reactions occur only at the melted electrode tip and in the hot weld pool immediately below the arc. The electrochemical reactions would result from ionic conduction of a portion of the welding current through the molten slag layer. Therefore, only thermochemical reactions are expected to occur at the surface of the detached droplets and solidifying weld pool since these parts are no longer carrying current.

The most important chemical considerations for submerged arc welding include the control of oxygen, oxidation losses of alloy elements, and the pickup of undesirable elements from the slag. A number of investigations have been made concerning the interaction between the slag and the metal in submerged arc welding of steel. Most of these investigations were based solely on thermochemical reactions (Refs. 1-9), although lately a few investigators have considered the electrochemical reactions that occur when direct current is used in welding. Frost (Ref. 10) considered the different chemical effects at the anode and cathode in electroslag welding. Blander and Olson (Ref. 11) postulated an electrochemical mechanism for the alteration of weld metal chemistry in submerged arc welding.

KEY WORDS

Submerged Arc Welding
Weld Metal Composition
Electrochemical Reaction
Thermochemical Reaction
Chemical Analyses
SAW
Alloy Elements
Flux Composition
Electrode Composition
Welding Speed Effect

Electrochemical and Thermochemical Reactions

Electrochemical reactions could be an important factor governing the chemistry of weld metal in direct current welding. Electrochemical effects can occur at the interfaces of the slag with the hot weld pool and the melted electrode tip. The relative numbers of ions and electrons in the slag govern the importance of these effects, which could be major factors controlling weld metal chemistry. When liquid slag has an interface with the molten metal, the electrochemical reactions are relatively simple to understand. This type of interface is present in submerged arc welding. The possible anodic reactions include the oxidation of iron and alloy elements, and the discharge and pickup of oxygen anions from the slag

$$M\,(\text{metal}) + nO^{2-}\,(\text{slag}) = MO_n\,(\text{slag}) + 2ne^- \quad (1)$$

where M is iron or an alloy element at the electrode tip/slag or the weld pool/slag interface. Thus, substantial oxidation losses of alloy elements and pickup of oxygen are expected at the anode. The

J. H. KIM, R. H. FROST and D. L. OLSON are with the Center for Welding Research, Department of Metallurgical Engineering, Colorado School of Mines, Golden, Colo. M. BLANDER is with Argonne National Laboratory, Chemical Technology Division/Materials Science and Technology Program, Argonne, Ill.

Paper presented at the 68th Annual AWS Meeting, held March 22-27, 1987, in Chicago, Ill.

Table 1—Compositions of Steel Plate and Welding Wire (wt-%)

Elements	Steel Plate	Welding Wire
C	0.18	0.059
Mn	1.25	1.38
Si	0.05	0.05
Mo	0.03	0.33
Cr	0.077	0.073
Ni	0.06	0.11
Al	0.004	0.018
Cu	0.036	0.77
Ti	0.001	0.033
P	0.018	0.012
S	0.031	0.015
O	0.002	0.002
N	0.004	0.004
Fe	balance	balance

possible cathodic reactions include reduction of metallic cations from the slag and, to some extent, the refining of nonmetallic elements such as oxygen and sulfur

$$M^{2+}\ (slag) + 2e^- = M\ (metal) \quad (2)$$

$$Si^{4+}\ (slag) + 4e^- = Si\ (metal) \quad (3)$$

$$O\ (metal) + 2e^- = O^{2-}\ (slag) \quad (4)$$

where M and Si represent electrodeposited metals at the interface. The large disparity in areas between the electrode tip and the weld pool results in different current densities. Current density is much higher at the electrode tip interface than at the weld pool interface. Thus, reactions at the electrode tip may exert a greater influence on the final weld metal chemistry than those at the weld pool.

In addition to the electrochemical reactions, thermochemical reactions also play an important role in controlling the weld metal chemistry in submerged arc welding. The thermochemical reactions occur very rapidly because of high temperature. These thermochemical reactions include deoxidation reactions, such as those encountered in steel making, and reactions that lead to a closer approach to equilibrium between the flux and metal phase. Examples of such reactions would be silicon pickup from a high silica flux or the oxidation loss of transition elements through a deoxidation reaction.

$$SiO_2\ (slag) + 2M\ (metal) = Si\ (metal) + 2MO\ (slag) \quad (5)$$

$$FeO\ (slag) + M\ (metal) = Fe\ (metal) + MO\ (slag) \quad (6)$$

where M can be aluminum or calcium in Reactions 5 and 6 and manganese in Reaction 6 for the flux system used in this research. The droplet forms at the electrode tip and then travels through the molten flux and plasma. The entire process occurs in a few milliseconds (Refs. 12, 13), and the temperature of the droplet is very high. Due to the high temperature, it is thermodynamically possible for chemical reactions to occur. A number of investigations have been made concerning the nature of chemical reactions at the melted electrode tips and the detached droplets (Refs. 5, 8, 12–18), and several investigators indicated that oxygen was transferred to the metal in these two zones (Refs. 2, 3, 13, 14, 18). In the hot weld pool immediately below the arc, the detached droplets become "diluted" with molten metal from the base plate. Although the slag/metal interfacial contact area available for reaction is much smaller than that of the detached droplets, the strong turbulance existing in the hot weld pool creates an effective stirring of the liquid metal. Moreover, pickup of oxygen at this zone is favored by the increased time available for reaction. It is believed that the pickup of oxygen is the result of the oxygen solubility being exceeded in the hot weld pool. The zone of the molten weld pool behind the electrode starts to cool and solidify as the electrode moves away from it. Upon cooling of the metal in the weld pool from a high temperature to the solidification temperature, a supersaturation with respect to silicon and manganese deoxidation reactions occurs initially. Therefore, silicon and manganese will react with dissolved oxygen, and then the composition will move rapidly towards equilibrium.

Figure 1 shows the schematic of expected variations in oxygen and silicon contents for an electrode-positive (reverse polarity) submerged arc weld due to electrochemical and thermochemical reactions. The curve shows the oxygen and silicon contents of steel in equilibrium with solid silica at some temperature. Before experiments were done, the composition variation was expected to follow the straight lines for an electrode-positive submerged arc weld. The anodic reaction at the melted electrode tip causes some oxygen pickup and silicon loss. The thermochemical reactions cause more oxygen pickup at the melted electrode tip and the detached droplet while the droplet is passed through the molten flux. At the cathodic weld pool, oxygen refining and silica reduction were expected, and then weld composition would vary with travel speed due to the difference in the amount of thermochemical deoxidation reaction. As the welding speed decreases, the amount of thermochemical deoxidation reaction increases because the heat input and the solidification time increase. Therefore, weld pool composition was expected to go to equilibrium composition as the travel speed decreases.

Experimental Procedure

Direct current electrode-negative (straight) and direct current electrode-positive (reverse) polarity submerged arc welds were made with 2.38 mm ($^3/_{32}$ in.) commercial low-carbon steel welding wire on ASTM A36 steel plates and a water-cooled pure copper plate. The compositions of the steel plate and the welding wire are given in Table 1, and the composition of the commercial flux used is shown in Table 2.

Figure 2 is a schematic drawing of a cross-section of the submerged arc welding process showing the melted electrode tips, the detached droplets and the base plate for both electrode-positive and electrode-negative polarities. The melted electrode tips, detached droplets and weld metal were collected and analyzed. The water-cooled copper plate was used as a base plate to collect the melted electrode tips and the detached droplets. The welding process was operated at a constant welding current of 585 A and a constant potential of 28.5 V. The constant current

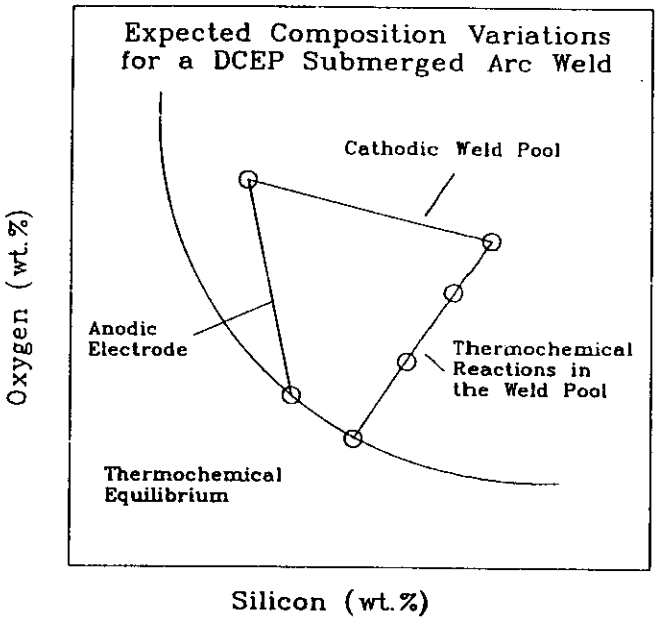

Fig. 1—Schematic of expected variations in oxygen and silicon contents for an electrode-positive polarity submerged arc weld.

Table 2—Composition of Welding Flux (wt-%)

Substance	Amount
SiO_2	11.22
Al_2O_3	18.14
MgO	33.23
CaF_2	25.26
CaO	6.92
MnO	1.15
TiO_2	0.90
Na_2O_3	0.82
Fe_2O_3	1.99
C	0.37

was obtained by adjusting the electrode velocity, which was 72 mm/s (170 in./min) for the anodic wire, and 99 mm/s (235 in./min) for the cathodic wire.

The electrode tips were collected by stopping the welding process, pulling the electrode away from the weld pool and cutting off the tip. The liquid metal droplets are released from the electrode tip and travel through the molten flux. The detached droplets were collected from welds made at a high velocity over a water-cooled copper plate so that the droplets are suspended in the molten flux. The detached droplets were extracted from the ground slag by magnetic separation. The speed of quenching attained is sufficient to freeze the metal composition established at high temperature. Single pass, bead-on-plate welds were made on steel plates at several welding speeds (1.55–34.67 mm/s) with constant voltage (28.5 V) and current (580 A) for both polarities. The wire feed speed was adjusted to maintain the constant current.

Analyses for oxygen were carried out using a LECO interstitial analyzer, *i.e.*, fusion in a graphite crucible under inert atmosphere. A Baird–Atomic emission spectrometer was used to determine manganese, silicon and other alloy elements in weld metals, welding wire and electrode tips. The electrode tips and wires were flattened in a rolling mill to get enough area for analysis. The detached droplets were analyzed using the wavelength dispersive analyzer on a JEOL scanning electron microscope.

A metallurgical model by Their (Ref. 5) is adopted to show the extent of element transfer between the weld metal and flux. Its application gives quantitative data for the gain or loss of elements arising from slag/metal reactions. The transfer efficiency into the weld can be expressed in terms of the difference between analytical and nominal compositions. The difference between analytical and nominal compositions is defined as delta (Δ) quantity. The analytical composition is obtained by chemical analysis methods and the nominal composition can be obtained by calculations based on the detached droplet and plate compositions and dilution. A positive concentration change ($\Delta > 0$) indicates a gain or pickup of a particular element, *i.e.*, transfer of element from the slag to the weld metal. A negative change ($\Delta < 0$) indicates a loss, *i.e.*, transfer from the weld metal to the slag.

Results and Discussion

The purpose of this investigation is to consider the relative influence of thermochemical and electrochemical reactions on the weld metal chemistry. Electrochemical reactions are expected because of the high current densities, and thermochemical reactions are expected because of the high temperature and the generally large temperature-dependent differences in chemical potentials of the various reactants and products in the flux and metal phases.

An examination of the welding wire, steel plate and flux compositions in Tables 1 and 2 shows that the wire and steel plate have very low silicon and oxygen concentrations, and a relatively high manganese concentration, while the flux has a high silica activity and a relatively low manganese-oxide/iron-oxide ratio, which is far from equilibrium with the welding wire and steel plate. Thus, the manganese content of the welding wire and steel plate would be expected to drop as a result of thermochemical oxidation losses to the flux, and the silicon and oxygen content would be expected to increase because of the reaction with the flux.

The reactions at the melted electrode tip, the detached droplet and the weld pool were considered. The chemical analysis results show that a substantial difference exists between the chemistries of anode and cathode. These differences are the result of electrochemical reactions.

Figure 3 shows the plot of the average oxygen contents of the welding wire, the melted electrode tips, and the detached droplets for both electrode-negative and electrode-positive polarity welding modes. This plot shows a very low oxygen content in the welding wire (20 ppm) and a very significant oxygen pickup in the melted electrode tips for both polarities. The influence of thermochemical oxygen pickup is shown by the fact that significant oxygen pickup is observed in both electrode-positive and electrode-negative configurations. This excess oxygen came from the surrounding atmosphere and decomposition of oxide components in the flux. The influence of electrochemical reactions is shown by the fact that the oxygen content of the anode in the electrode-positive polarity power mode (591 ppm) is over twice that of the cathode in the electrode-negative polarity power mode (277 ppm). This oxygen content difference is due to oxygen pickup at the anode and oxygen refining at the cathode. The real difference is somewhat less since more wire is fed and melted at the cathode for a fixed current, thus diluting the total electrochemical and thermochemical effect at the cathode. If the electrochemical and thermochemical reactions were considered as separate steps, the average melted electrode tip oxygen concentration for the two polarities could be considered to crudely represent the thermochemical contribution, and the separation of two concentrations from this mean would represent the electrochemical effects. However, the different wire feed rates cloud this interpretation. After the

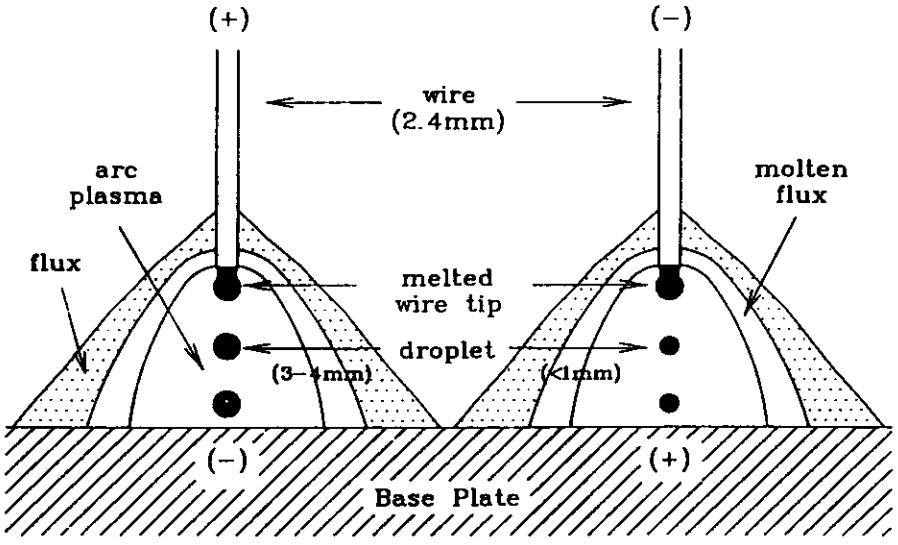

Fig. 2—Schematic of the cross-section of a submerged arc welding process showing the melted welding wire tips, the detached droplets and the base plate for both electrode-positive and electrode-negative polarities.

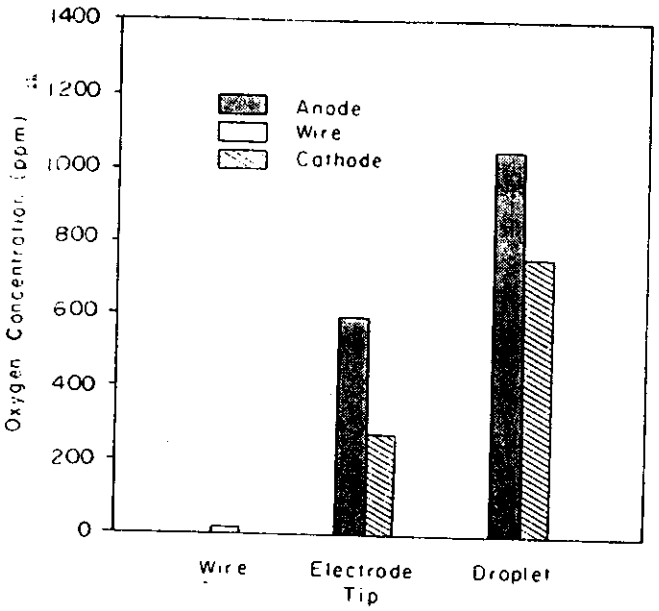

Fig. 3 – Average oxygen contents of the welding wire, the electrode tips and the detached droplets for both electrode-negative (cathodic wire) and electrode-positive (anodic wire) polarities.

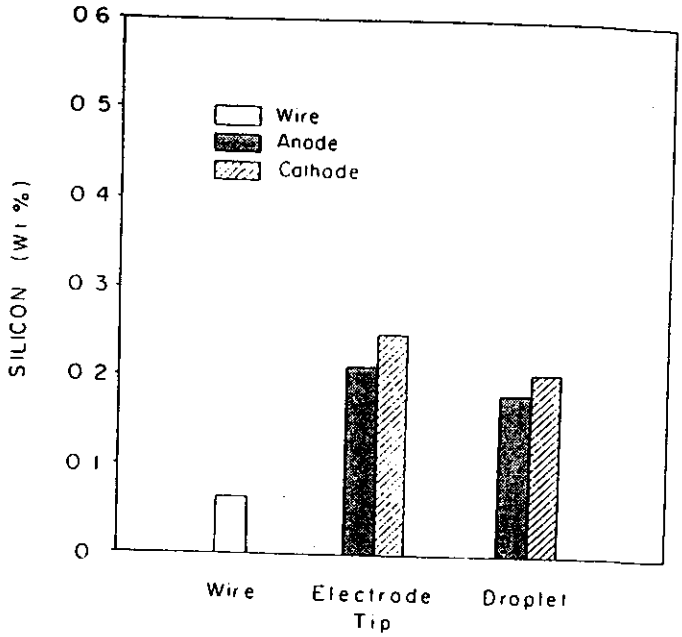

Fig. 4 – Average silicon contents of the initial wire, the electrode tips, and the detached droplets for both electrode-negative (cathodic wire) and electrode-positive (anodic wire) polarities.

molten droplet separates from the wire, the electrochemical reaction ceases. But the thermochemical reaction continues while the droplet is falling through the molten slag. Therefore, the detached droplet shows higher oxygen content than the melted electrode tip due to the increase in oxygen content by the continuous decomposition of flux. Even though electrochemical reaction does not occur in detached droplets, the results of oxygen analysis still show the electrochemical reaction effect at the melted electrode tips as indicated by the difference in oxygen contents between anodic and cathodic droplets.

Figures 4 and 5 show the average silicon and manganese contents in the initial electrode, the melted electrode tip and the detached droplet. The melted electrode tips show the increases in silicon concentration (less increase at the anode and more increase at the cathode) and the decreases in manganese concentration (less decrease at the cathode and more decrease at the anode) for both polarities. This is evidence that both thermochemical and electrochemical reactions occurred at the melted electrode tip. The initial welding wire has a very low silicon content, while the flux has a high silicon-oxide content. This causes the thermochemical pickup of silicon from the flux. The electrochemical influence is significant, as indicated by the fact that the cathodic electrode tip silicon content is about 0.06 wt-% higher than that of the anodic electrode tip, and by the fact that the cathode feed rate is higher than the anode feed rate, which means the total amount of silicon in the cathodic electrode tip is relatively higher than indicated in Fig. 4. Both thermochemical and electrochemical reactions are also indicated in the case of manganese; however, the high manganese content in the electrode and the low manganese-oxide (MnO)/iron-oxide (Fe_2O_3) ratio in the flux lead to thermochemical manganese loss at the melted electrode tip. Therefore, manganese oxidation and silicon reduction reactions are major thermochemical reactions in this system. The changes in the silicon and manganese concentrations from the electrode tip to the detached droplet are mostly thermochemical. With silicon, however, there is a decrease rather than an expected increase in silicon content of the detached droplet compared to the melted electrode tip, indicating that a large fraction of the silicon in the droplet has back reacted with more noble metal oxides in the flux (*e.g.*, Fe_2O_3). One of the possible driving forces for this reaction is related to the possibility that the droplet is at a lower temperature and has a higher oxygen content than the tip. The average manganese content is further decreased by thermochemical reactions with more noble metal oxides in the flux when going from the electrode tip to the detached droplet, which falls through and reacts with the flux.

Figure 6 compares the detached droplet compositions for the various alloy elements. Silicon, aluminum and manganese

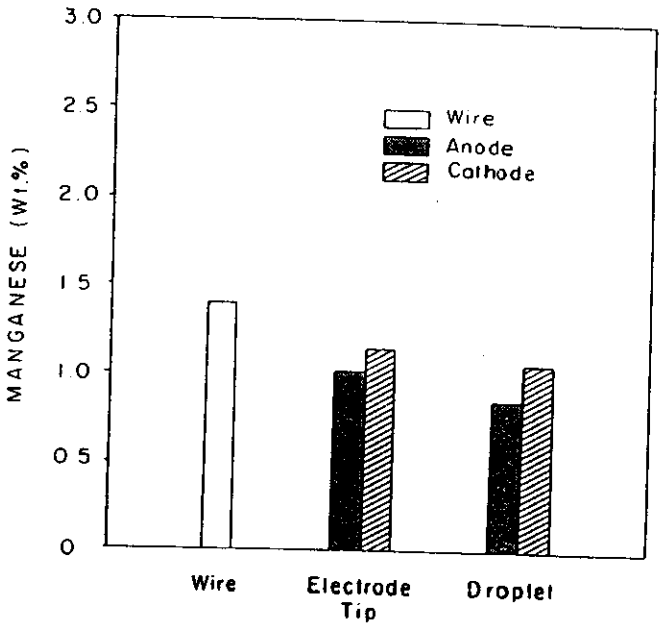

Fig. 5 – Average manganese contents of the initial wire, the electrode tips and the detached droplets for both electrode-negative (cathodic wire) and electrode-positive (anodic wire) polarities.

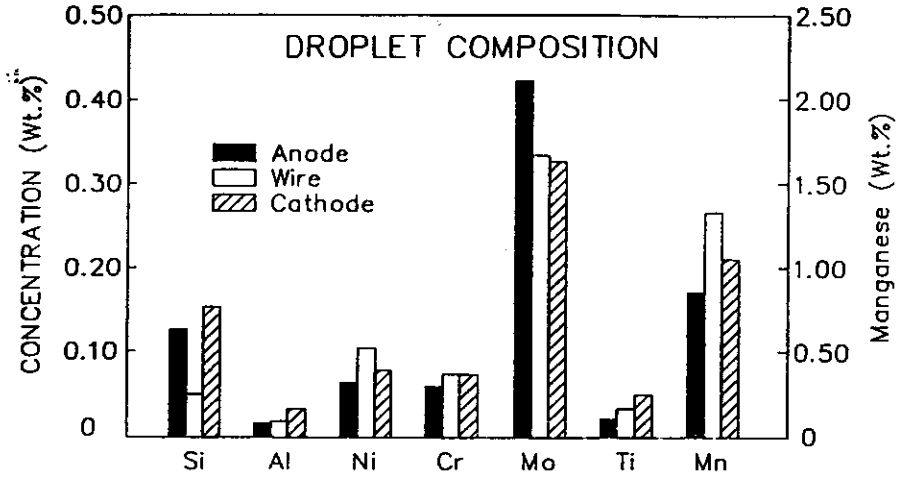

Fig. 6 – Average droplet compositions for silicon, aluminum, nickel, chromium, molybdenum, titanium and manganese for electrode-negative and electrode-positive polarities compared with the initial welding wire compositions.

show higher concentrations in the cathodic droplets than in the anodic droplets. This is largely caused by oxidation losses to the flux at the anode and electrochemical reduction from the flux at the cathode during the reaction at the melted electrode tip. The differences for nickel, titanium and chromium are of the order of the analytical uncertainties and are thus inconclusive. Molybdenum shows the opposite trend. That is, the concentration in the anode is higher than that of the cathode. This behavior is difficult to explain in terms of molybdenum reaction alone, but if iron reaction is also taken into account, it can be explained easily. Iron is the major electrode constituent and it is more easily oxidized than molybdenum. Therefore, the loss of iron at the anode and the gain of iron at the cathode are relatively greater than those of molybdenum, and these cause an increase in molybdenum concentration at the anode and a decrease at the cathode. Thus, this behavior of molybdenum is also the result of electrochemical reaction.

Figures 7 through 14 show the results of chemical analyses of the anode and cathode weld metal for silicon, manganese, aluminum, molybdenum and oxygen as a function of welding speed. The results for the anode and cathode of each element are plotted together. These results show that electrochemical reactions cause substantial changes in weld metal chemistry.

Figure 7 illustrates the variations in delta silicon due to polarity. High transient concentration of oxygen may exist in the liquid metal at the hot weld pool as a result of high solubility at elevated temperature. On slow cooling down to the solidification temperature, this will lead to spontaneous reaction and losses of dissolved silicon. The silicon loss must be due to the formation of some deoxidation reaction product. It is generally accepted that formation of silicon oxide (SiO_2) takes place when sufficient oxygen is available. But silicon loss is recovered by electrochemical reduction reaction at the cathode and increased at the anode by electrochemical oxidation reaction. Therefore, silicon shows much loss at the anode, and a little gain or almost no change at the cathode.

Figure 8 shows the variations in delta manganese due to polarity. Similar to silicon, oxidation of manganese is favored by the lower temperature prevailing in the cooler part of the weld pool. Here, manganese will react with dissolved oxygen to form slags that exhibit a large loss of manganese in both anode and cathode weld metal. The reason why manganese shows extensive losses in both cases is because the flux has a little manganese oxide (MnO) and the base plate has a high manganese content. Therefore, manganese can be oxidized easily. Another reason for manganese loss can be a result of the evaporation because vapor pressure increases strongly with temperature. But the difference in delta manganese due to polarity shows the effect of electrochemical reaction. That is, the cathode shows less loss than the anode because of the electrochemical reduction reaction at the cathode, and the electrochemical oxidation reaction at the anode.

Variations in delta aluminum are shown in Fig. 9. Aluminum, like silicon and manganese, is also oxidized while the temperature of the weld pool is lowered to the

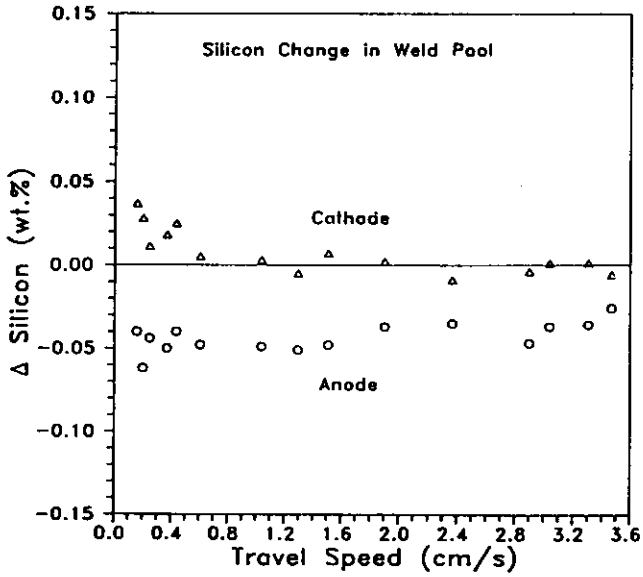

Fig. 7 – Gain or loss of silicon due to the reactions in the weld pool for electrode-negative and electrode-positive polarities as a function of welding speed.

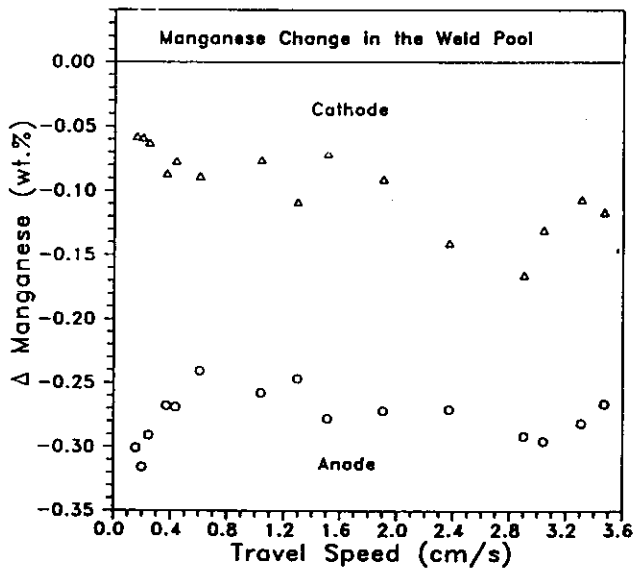

Fig. 8 – Gain or loss of manganese due to the reactions in the weld pool for electrode-negative and electrode-positive polarities as a function of welding speed.

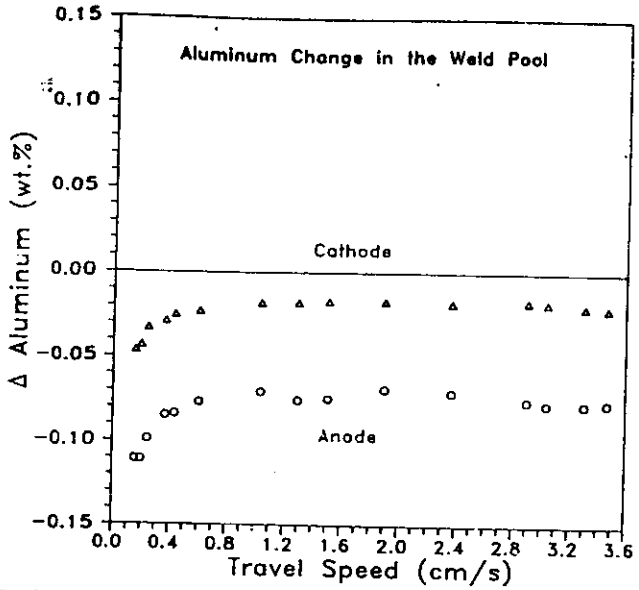

Fig. 9 – Gain or loss of aluminum due to the reactions in the weld pool for electrode-negative and electrode-positive polarities as a function of welding speed.

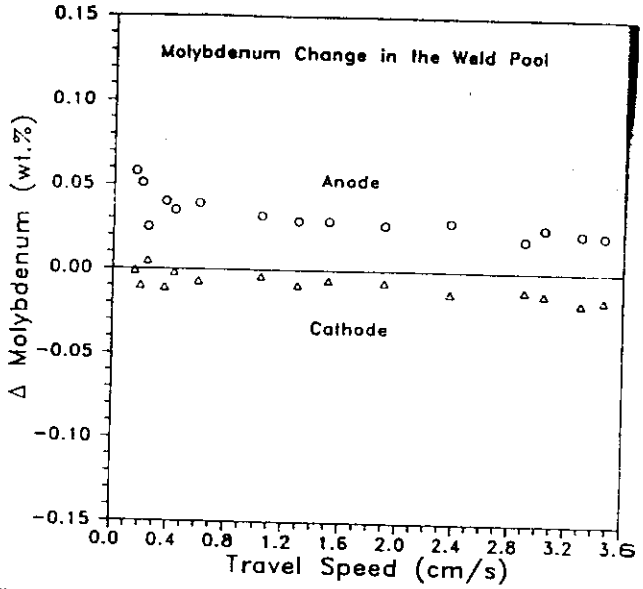

Fig. 10 – Gain or loss of molybdenum due to the reactions in the weld pool for electrode-negative and electrode-positive polarities as a function of welding speed.

solidification temperature. Aluminum oxide (Al_2O_3) is stable at high temperature rather than silicon oxide (SiO_2) and manganese oxide (MnO), as indicated in the Ellingham diagram. Therefore, even though the flux contains a large amount of aluminum oxide, it is difficult to pick up the aluminum from the slag by electrochemical reduction reaction at the cathode weld pool. So, the results show the aluminum losses even at the cathode weld pool. But the lesser loss at the cathode is the evidence for the electrochemical reaction.

Figure 10 shows the variations in delta molybdenum due to polarity. Molybdenum changes show the opposite trend as in the melted electrode tip. This behavior of molybdenum is the result of iron losses at the anode and pickup at the cathode as discussed previously.

Figures 11 through 13 show the variations in delta nickel, chromium and titanium due to polarity. Those elements also show a little electrochemical effect. But the differences between anode and cathode are of the order of the analytical uncertainties and are thus inconclusive.

Figure 14 shows the variations in delta oxygen due to polarity. Oxygen losses are shown at both cathode and anode, and the cathode shows less loss than the anode. This is the result of the difference in the slag/metal interfacial contact area available for deoxidation reaction. The area of the cathode is smaller than that of the anode. Therefore, the separation of deoxidation products at the anode is easier than that at the cathode. Thus, electrochemical effect may be swept out by thermochemical reaction.

Figure 15 is the composition map for both electrode-negative and electrode-positive polarity submerged arc welding, showing the variations in oxygen and silicon contents during welding. The curves are the plots of the silicon and oxygen contents of steel in equilibrium with solid

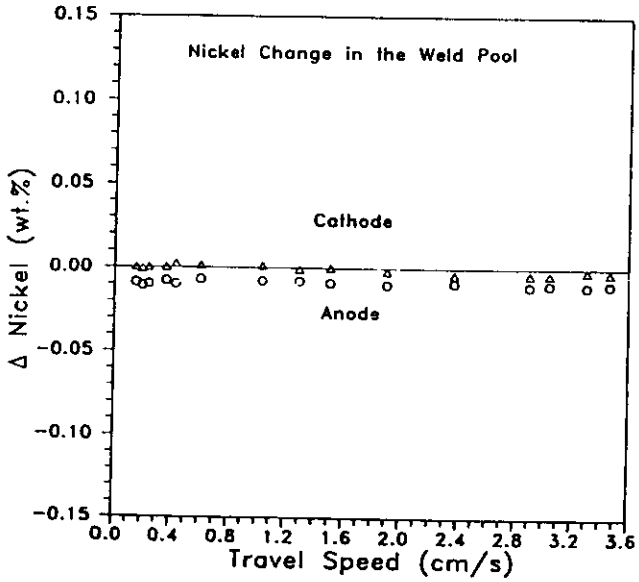

Fig. 11 – Gain or loss of nickel due to the reactions in the weld pool for electrode-negative and electrode-positive polarities as a function of welding speed.

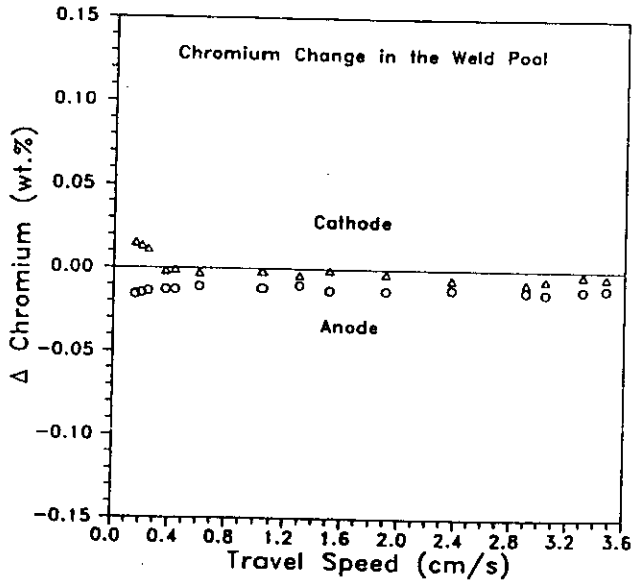

Fig. 12 – Gain or loss of chromium due to the reactions in the weld pool for electrode-negative and electrode-positive polarities as a function of welding speed.

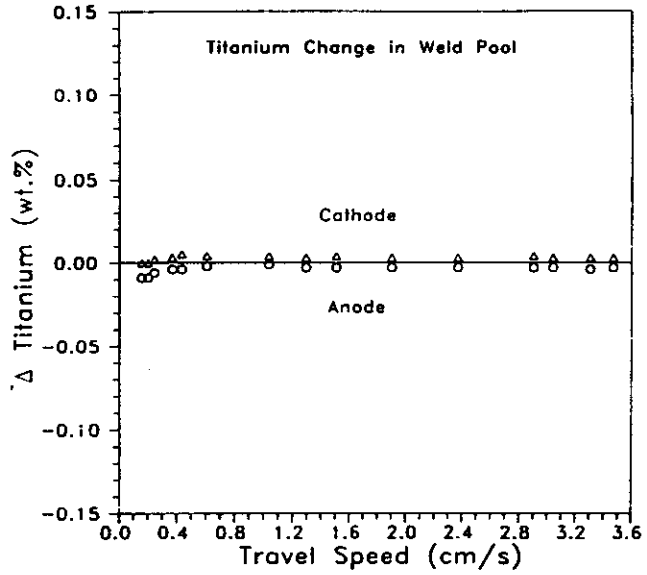

Fig. 13 – Gain or loss of titanium due to the reactions in the weld pool for electrode-negative and electrode-positive polarities as a function of welding speed.

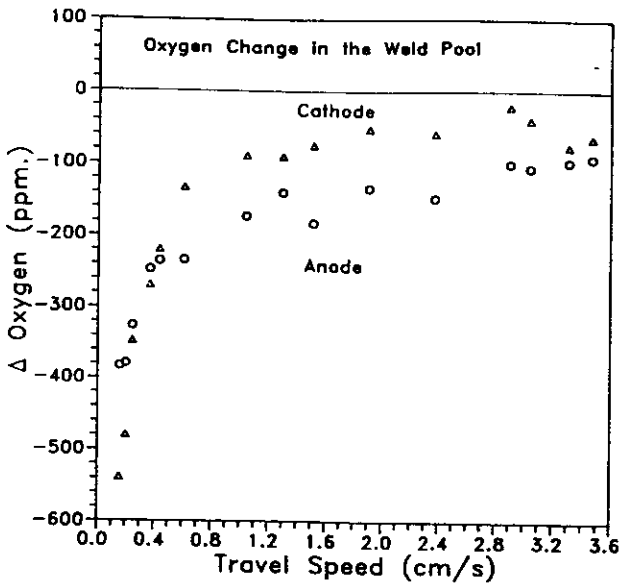

Fig. 14 – Gain or loss of oxygen due to the reactions in the weld pool for electrode-negative and electrode-positive polarities as a function of welding speed.

silica at 1600°C (2912°F) and 1800°C (3272°F). The compositions of welding wire, melted electrode tips, detached droplets and weld metal are plotted on the diagram for both polarities. The wire has low silicon and oxygen contents. Both anodic and cathodic electrode tips show an increase in silicon content due to the oxidation of iron and manganese, and in oxygen content due to decomposition of flux and contamination from the atmosphere. But the cathodic electrode tip shows a greater increase in silicon and less increase in oxygen, due to the electrochemical silicon reduction and oxygen refining reactions. While the detached droplets are falling through the molten flux, the droplets pick up the oxygen by flux decomposition and contamination from the atmosphere. Therefore, the oxygen contents in the droplets are higher than those in the electrode tips for both polarities. The weld metal shows decreases in silicon and oxygen contents by deoxidation reaction and composition variation due to welding speed. As the welding speed decreases, the composition of the weld metal approaches the equilibrium composition.

Conclusions

1) Both electrochemical and thermochemical reactions are significant in submerged arc welding.

2) The thermochemical reactions move the flux and weld metal compositions toward chemical equilibrium. In this study, manganese activity was higher in the metal than in the flux; therefore, manganese oxidation loss from the metal to the flux was observed. Silicon activity was higher in the flux; therefore, a thermochemical silicon pickup by the weld metal was observed.

3) The electrochemical reactions at the anode include oxidation losses of alloy elements to the flux and the discharge and pickup of oxygen anions from the flux. The electrochemical reactions at the cathode include the reduction of metal ions from the flux and the refining of oxygen.

4) Thermochemical and electrochemical composition changes are greater at a low than at a high welding speed. Electrochemical reactions are enhanced by higher, total current flow per unit volume of weld metal. Thermochemical reactions at a low welding speed are enhanced by higher temperatures and longer reaction time before solidification.

5) Composition paths for the silicon-oxygen equilibrium are different for direct current electrode-positive (reverse polarity) and direct current electrode-negative (straight polarity) welds.

6) The total gain or loss of alloy elements in weld metal is influenced by the compositions of flux, electrode and base plate, and by welding process conditions.

Further experiments with synthetic fluxes, which are chosen to minimize thermochemical reactions, are planned and should help to better define the relative importance of electrochemical reactions.

Fig. 15 – The composition map for direct current electrode-negative (DCEN) and direct current electrode-positive (DCEP) polarity submerged arc welding showing the variations in oxygen and silicon contents during welding.

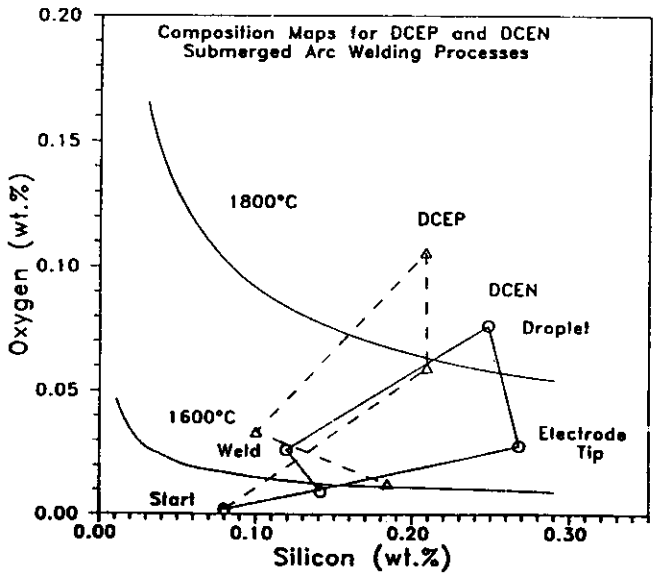

Acknowledgments

J. H. Kim, R. H. Frost and D. L. Olson wish to acknowledge the support of the U.S. Army Research Office at the Colorado School of Mines, and M. Blander acknowledges the support of the Office of

Naval Research at Argonne National Laboratory under Navy Order No. N00014-85-F-0097.

References

1. Belton, G. R., Moore, T. J., and Tankins, E. S. 1963. Slag-metal reactions in submerged-arc welding. *Welding Journal* 42(7): 289-s to 297-s.

2. Chai, C. S., and Eagar, T. W. 1982. Slag-metal reactions in binary CaF_2-metal oxide welding fluxes. *Welding Journal* 61(7): 229-s to 232-s.

3. Chai, C. S., and Eagar, T. W. 1981. Slag-metal equilibrium during submerged arc welding. *Metall. Trans. B* 12B(9): 539 to 547.

4. Indacochea, J. E., Blander, M., Christensen, N., and Olson, D. L. 1985. Chemical reactions during submerged arc welding with FeO-MnO-SiO_2 fluxes. *Metall. Trans. B* 16B(6): 237 to 245.

5. Their, H. 1980. Metallurgical reactions in submerged arc welding. *Proc. Intl. Conf. on Weld Pool Chemistry and Metallurgy.* The Welding Institute, London, England, pp. 271 to 278.

6. North, T. H., Bell, H. B., Nowicki, A., and Craig, I. 1978. Slag/metal interaction, oxygen and toughness in submerged arc welding. *Welding Journal* 57(3): 63-s to 75-s.

7. Davis, M. L. E., and Coe, F. R. 1977. The chemistry of submerged arc welding fluxes. The Welding Institute. 39/1977/M.

8. Mitra, U. 1984. Kinetics of slag metal reactions during submerged arc welding of steel. Ph.D. dissertation. MIT, Cambridge, Mass.

9. Blander, M., and Olson, D. L. 1984. Thermodynamic and kinetic factors in the pyrochemistry of submerged arc flux welding of iron-based alloys. Proc. Intl. Symp. on Metallurgical Slags and Fluxes. The Met. Soc. of AIME.

10. Frost, R. H., Olson, D. L., and Edwards, G. R. 1983. The influence of electrochemical reactions on the chemistry of the electroslag welding process. Engineering foundation conferences. *Modeling of Casting and Welding Processes II.* eds. J. A. Dantzig and J. T. Berry. The Met. Soc. of AIME.

11. Blander, M., and Olson, D. L. 1986. Electrochemical effects on weld pool chemistry in submerged arc and D.C. electroslag welding. *Proc. Intl. Conf. on Trends in Welding Research.*

12. Pokhodnya, I. K., and Kostenko, B. A. 1965. Fusion of electrode metal and its interaction with the slag during submerged arc welding. *Avt. Svarka* 10: 16 to 22.

13. Potapov, N. N., and Lyubavski, K. V. 1971. Oxygen content of weld metal deposited by automatic submerged arc welding. *Svar. Proiz.* 1: 11 to 15.

14. North, T. H. 1977. The distribution of manganese between slag and metal during submerged arc welding. *Welding Research Abroad* 23: 2 to 13.

15. Potapov, N. N., and Lyubavski, K. V. 1971. Interaction between the metal and slag in the reaction zone during submerged arc welding. *Svar. Proiz.* 7: 9 to 11.

16. Norin, P. A., and Malyshev, N. I. 1982. Losses of manganese from electrode droplets in arc welding in air. *Svar. Proiz.* 2: 21 to 33.

17. Grong, O., and Christensen, N. 1982. Factors controlling weld metal chemistry. Final Report Contract No. DATA 376-81-C-0309. European Research Office of the U.S. Army.

18. Lau, T., Weatherly, G. C., and McLean, A. 1985. The source of oxygen and nitrogen contamination in submerged arc welding using $CaO-Al_2O_3$ based fluxes. *Welding Journal* 64(12): 343-s to 347-s.

Lecture 3

Electroslag Welding of an Advanced Double-Hull-Design Ship

Nonconsumable guide electroslag welding provides a highly cost-effective means to weld T-joints in double-hull ship construction

BY J. H. DEVLETIAN, D. SINGH AND R. B. TURPIN

Since Congress passed the Oil Pollution Act of 1990, all tankers entering U.S. harbors must have double hulls by the year 2010 (Refs. 1, 2). A typical double-hull design for an oil tanker or military ship has a greater number of hull-to-stiffener T-joints (Ref. 3) than a standard design, and these are ideal applications for electroslag welding (ESW). The fabrication of double hulls is extremely competitive (Refs. 4, 5) with nearly all current double-hull tanker fabrication being performed overseas. Although ESW was widely used in the construction of buildings (Ref. 6) and bridges (Ref. 7), it has seen limited applications in ship construction in this country (Refs. 8, 9).

Over the last two decades, many innovative improvements in consumable guide ESW were developed to improve the integrity and fracture toughness of electroslag welds for bridges and buildings. By incorporating a specially alloyed tubular filler metal and narrow groove techniques for reduced heat input, substantial improvements in both weld metal and HAZ toughness were achieved (Refs. 10–13). In 1995, Juers and McConnell developed a procedure to weld T-joints in a single pass using the electrogas process (Ref. 14). This welding was incorporated into the Navy's advanced double hull (ADH) design. These T-joints consisted of three orthogonal 25-mm (1-in.) thick plates of ABS CS grade steel and were joined by electrogas welding in a single pass with a commercial 3.2-mm (1/8-in.) diameter self-shielded welding wire.

The objective of this work was to demonstrate the cost-effectiveness and design acceptability of joining three 25-mm-thick structural steel plates in a T-joint configuration (similar to the ADH design) with a single full joint penetration uphill weld containing fillets using the nonconsumable guide ESW process. The weld metal property requirements are listed in Table 1.

Table 1—Weld Metal Property Requirements

Yield strength	345 MPa (50 ksi) min.
Tensile strength	490–650 MPa (70–95 ksi)
CVN toughness	20 J @ −18°C (15 ft-lbs @ 0°F)
CVN toughness (HAZ)	27 J (20 ft-lbs) @ −10°C (14°F)
Fatigue strength	AWS/AASHTO D1.5 Category B for nonredundant structures

Procedure

The nonconsumable guide ESW process was utilized to join two 25-mm-thick hull plates to a 25-mm-thick stiffener in a T-joint configuration as shown in Fig. 1. The weld joint cavity consisted of a 25 x 25 mm space between the three plates. The length of the weld was 2.4 m (8 ft) plus run-on and run-off tabs. The 25-mm-thick steel plates used included 1) dual-certified A36 and ABS Grade A and 2) ABS Grade CS with compositions given in Table 2. There were two water-cooled stationary shoes to form the two 6-mm (1/4-in.) fillets of the T-joint. To ensure smooth fillet formation, the stationary shoes were machined with a recess, which permitted only about 30% of the cooling shoe surface to contact the steel plate. In this way, the copper shoes would slowly extract heat to allow the fillets to fill and freeze with a smooth contour. Unlike commercial ESW systems, the snorkel or nozzle (Fig. 2) was not attached directly to the sliding shoe in order to adjust the sliding shoe and nozzle independently. The sliding shoe was machined to provide a 1.6-mm (1/16-in.) reinforcement on the flat face of the T-joint.

The power source for ESW was a 1500-A, 100% duty cycle, DC constant voltage machine used with electrode positive. Weld heat input averaged 25 kJ/mm (635 kJ/in.) using 700 A, 47 V and 76 mm/min (3 in./min). An automatic flux feeder was attached above the slag pool (shown in Fig. 2) to compensate for the thin layer of slag that was continuously consumed on the cold shoe surfaces during welding.

All-weld-metal tensile specimens and Charpy V-notch (CVN) impact toughness specimens were cut from the weld joint as shown in Fig. 3. In addition, nine 2.4-m-long electroslag welds were incorporated into a 6.4-m (21-ft) I-beam for fatigue testing. As shown in Fig. 4, each electroslag welded T-joint was fitted and submerged arc welded into a 21-ft-long I-beam for fatigue testing. The four-point bending fatigue test was designed to evaluate the electroslag weld joint performance in bending fatigue. Each beam was cyclically loaded with a single 489 kN (110 kips) digitally controlled, hydraulic actuator with an in-line 667 kN (150 kips) load cell. Each actuator was centered on 1.2-m (4-ft) spreader beams, which distributed the load equally to load points on the test specimen. The actuators were controlled by a computer to produce sinusoidal waveforms at

J. H. DEVLETIAN is Professor and R. B. TURPIN is Senior Research Engineer in the Dept. of Materials Science & Engineering, Oregon Graduate Institute, Portland, Ore. D. SINGH is Product Development Engineer, Stoody Company, Bowling Green, Ky.

Table 2—Compositions of Plate and Filler Metals

	ABS Grade Steels		Filler Metal		Weld Metal
	Grade A	Grade CS Fully Killed, Normalized	EWT-G Metal Cored Wire	E70S-3 Solid Wire	EWT-G deposited on Grade CS
C	0.13	0.12	0.034	0.11	0.089
Mn	1.1	01.3	1.2	1.12	1.23
Si	0.22	0.25	0.4	0.50	0.38
Ni			2.04		1.05
Mo			0.4		0.16
S	0.012	0.011	0.010	0.010	0.011
P	0.008	0.006	0.010	0.009	0.013
Al	0.04	0.05	0.02		0.024
Ti			0.06		0.03

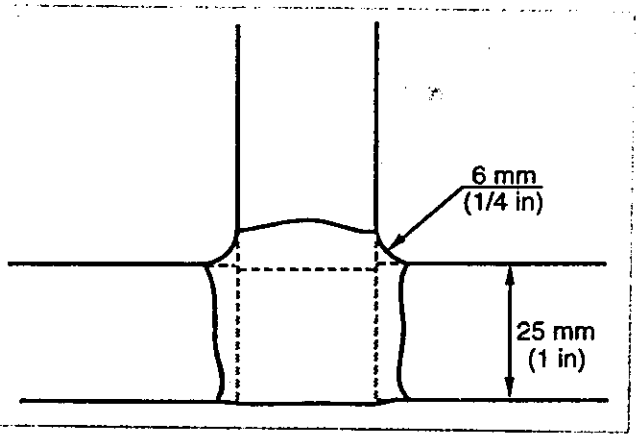

Fig. 1 — T-joint geometry for ESW three orthogonal 25-mm-thick steel plates.

frequencies from 1 to 3 hz, depending on the applied load range.

Tensile Properties of Weld Metal

The all-weld-metal tensile properties of the electroslag weld joint met the requirements of FES70-EWT-G category per AASHTO D1.5 and AWS D1.1, which specifies 345 MPa (50 ksi) minimum yield strength and 490–650 MPa (70–95 ksi) tensile strength. The actual tensile properties are given in Table 3. The average weld metal yield strength was 452 MPa (65.5 ksi) compared to the base metal yield strength of 283 MPa (41.1 ksi).

Table 3—Average Tensile Properties of CS Grade Base Metal and Weld Metal Deposited by ESW Using EWT-G Metal Cored Filler Metal

	Weld Metal 25 kJ/mm	Base Metal ABS Gr. CS
Yield strength		
MPa	452	283
(ksi)	(65.5)	(41.1)
Tensile strength		
MPa	647	454
(ksi)	(93.9)	(65.8)
% Elongation	27	30
% R.A.	51	54
Hardness, HRB	90	71

Table 4—CVN Toughness of Weld Metal and HAZ for Electroslag Welds Deposited with EWT-G Metal-Cored Filler Metal on 25-mm-Thick CS Grade Plate at Different Levels of Heat Input

	Average CVN Toughness at −10°C (14°F)		
	35 kJ/mm (890 kJ/in.)	31 kJ/mm (790 kJ/in.)	25 kJ/mm (640 kJ/in.)
Weld Metal			
Weld Center	52 J (38 ft-lbs)	67 J (49 ft-lbs)	87 J (65 ft-lbs)
1/4 Distance (See Fig. 5)	94 (69)	97 (71)	122 (90)
HAZ at mid thickness			
Weld interface	46 (34)	58 (43)	67 (49)
1 mm	45 (33)		
2 mm	45 (33)	48 (35)	57 (42)
Unaffected base metal		80 (59)	

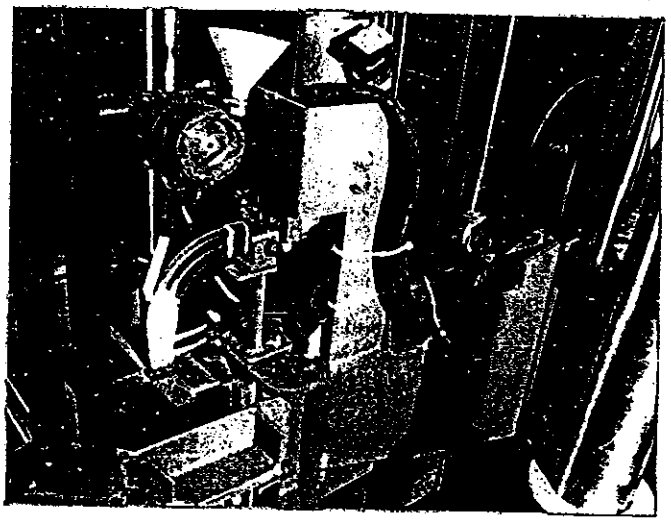

Fig. 2 — Top view of the nonconsumable guide ESW system to weld flange-to-web T-joints. Automatic flux feeding system is shown above the snorkel.

CVN Impact Toughness of Weld Metal and HAZ

The results of CVN toughness testing of the weld metal and HAZ, which included tests 1 and 2 mm from the weld interface, showed that the requirements for 20 J at −18°C (15 ft-lbs at 0°F) in the weld (Fig. 5) and 27 J at −10°C (20 ft-lbs at 14°F) in the HAZ (Table 4) were met. Furthermore, decreasing the heat input from 35 kJ/mm to 25 kJ/mm resulted in increasing CVN toughness for both the weld metal and the HAZ. As shown in Table 4, the CVN toughness of the EWT-G weld metal deposited at 25 kJ/mm exceeded that of the unaffected base metal. Although the HAZ exhibited the lowest CVN toughness values, these values were still well above that required by the ABS Grade CS specification.

The CVN transition curves for the weld metal (shown in Fig. 5) illustrate the superior toughness of the Mn-Ni-Mo steel tubular filler metal (EWT-G) over the conventional mild steel (E70S-3) solid filler metal. Since dilution of the weld metal by the ABS Grade CS base metal approached 50%, the Mn-Ni-Mo filler metal wire provided the means to improve CVN toughness of the weld metal. The reason for the excellent CVN toughness is the low heat input and the favorable microstructure.

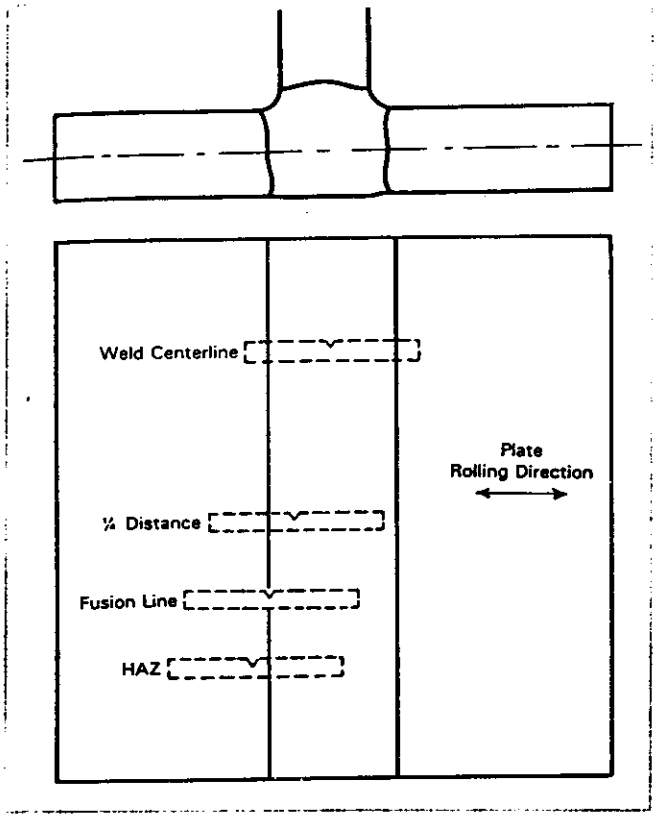

Fig. 3 — Locations of Charpy V-notch toughness specimens of the weld metal and HAZ extracted from the mid-thickness of electroslag welded T-joints.

Fatigue Properties

Nine full size I-Beams were fabricated out of the 2.4-m-long electroslag welded T-joint as shown in Fig. 4. In this figure, the electroslag-welded T-joint is the web-to-flange portion of the I-beam. Beams were tested at three stress range levels: 138, 207, and 276 MPa (20, 30, and 40 ksi). For example, using a stress range of 138 MPa (20 ksi), the maximum stress was +10 ksi (69 MPa) in tension to –10 ksi (–69 MPa) in compression for a maximum of 2 million Hz. In all cases, the beams containing the flange-to-web T-joints passed the Navy's stringent requirements for fatigue. These requirements include passing the Category B criteria of both AWS D1.1 *Structural Welding Code — Steel* (Ref. 6) and AASHTO/AWS D1.5 *Bridge Welding Code* (Ref. 7)

Resistance to Solidification Cracking

Despite the fast welding speeds of 76 mm/min (3 in./min) and low heat input of 25 kJ/mm (635 kJ/in.), the weld metal exhibited excellent resistance to solidification cracking. The factors promoting the resistance to cracking were 1) filler metal composition (containing very low carbon with Mn-Ni-Mo alloying) to produce an equiaxed grain structure at the weld centerline, and 2) a tubular filler metal to reduce the depth/width ratio of the weld pool. Ultrasonic testing and metallographic sections of weld joints showed no evidence of cracking. A weld joint cross-section is shown in Fig. 6.

Microstructure of Weld

The microstructure of weld metal deposited on Grade CS steel with E70S-3 solid wire (Fig. 7) contained very little acicular ferrite. Thus, the CVN toughness values for the E70S-3 weld metal were less than those for the EWT-G weld metal (Fig. 5), which contained a mixture of acicular ferrite and low-carbon

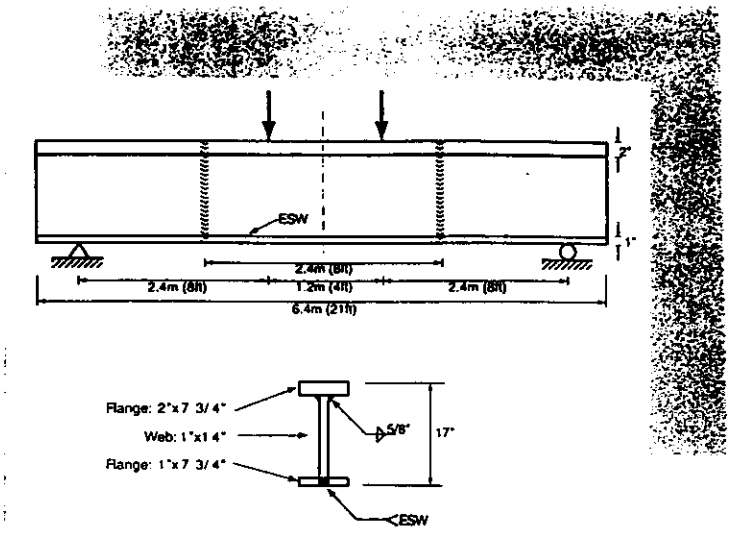

Fig. 4 — Fatigue test setup to evaluate the web-to-flange electroslag weld T-joint.

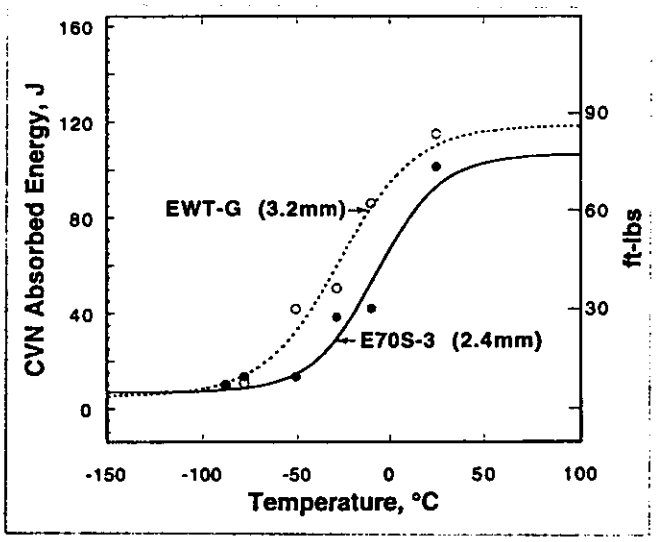

Fig. 5 — Charpy V-notch toughness transition curves for weld metal (centerline location) deposited on ABS Grade CS steel by ESW at 25 kJ/mm.

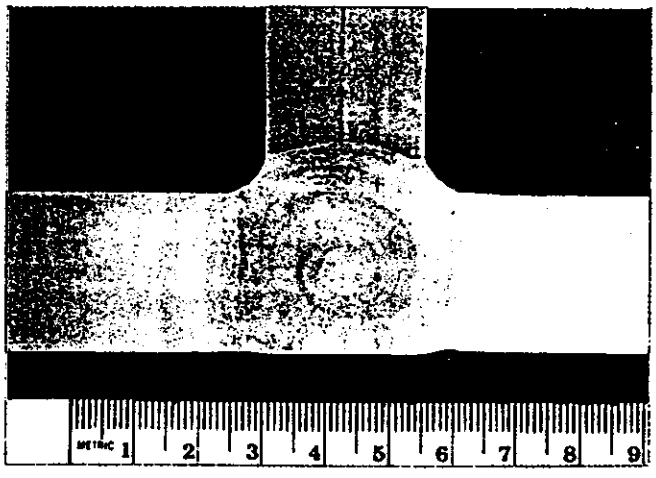

Fig. 6 — Etched cross-section of T-joint deposited by ESW.

Fig. 7 — Microstructure of weld metal deposited by ESW at 25 kJ/mm using E70S-3 filler metal. 400X.

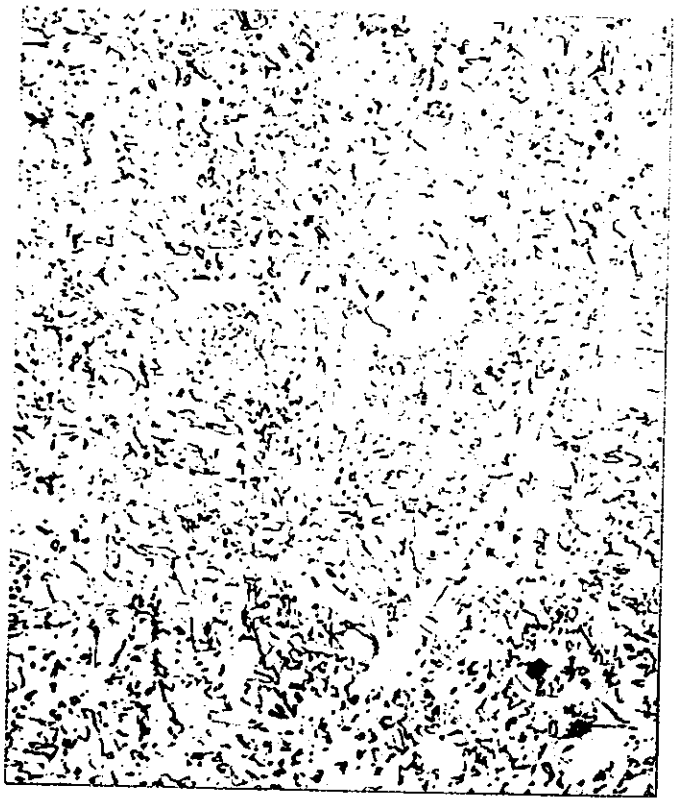

Fig. 8 — Microstructure of weld metal deposited by ESW at 25 kJ/mm using EWT-G filler metal. 400X.

bainite as shown in Fig. 8. The EWT-G wire was designed with Mn, Ni and Mo and very low carbon to produce electroslag weld metal containing a mixture of tough acicular ferrite and bainite. Furthermore, the addition of Mn, Ni and Mo in the tubular filler metal virtually eliminated the occurrence of grain boundary ferrite — Fig. 8. The use of the EWT-G wire appears to be ideally suited for electroslag welding of mild steels.

Economy of Electroslag Welding

Electroslag welding should be of interest to commercial shipbuilders as well as heavy-section steel fabricators because ESW represents a substantial cost savings over conventional arc welding processes. For example, similar welds deposited in a T-joint configuration by FCAW and SAW would require at least 18 passes and 7 passes (Ref 14), respectively, compared to a single full joint penetration pass by ESW. The deposition rate for ESW of the T-joint was approximately 50 lb/h, while the rates for FCAW and SAW were 7 and 15 lb/h, respectively (Ref 14). Since the entire ESW system (siding shoe, flux feeder, power input, etc.) are all electrically controlled, the process can be fully automated with little additional effort. With respect to the shop environment, the ESW process is noiseless and smokeless.

Conclusion

Weld metal deposited by nonconsumable guide ESW of 25-mm-thick ABS Grade A and Grade CS steel plates in a T-joint configuration meets all the requirements of ABS, AASHTO and AWS. Electroslag welding is a viable and cost-effective welding process for construction of double-hull structures.

Acknowledgments

The authors are grateful to the Navy Joining Center for supporting this project and to Ray Juers of Naval Surface Warfare Center for his guidance. The authors are also grateful to Stoody Co. for providing tubular filler metals.

References

1. Tankers playing by uncle's rules. Aug. 1992. *Marine Log*, pp. 50–55.

2. Greening the world tanker fleet. Sept. 1991. *Marine Log*, pp. 37–43.

3. Beach, J. E. 1991. Advanced surface ship hull technology — cluster B. *Naval Engineers Journal*, pp. 27–37.

4. Frankel, E. G. 1996. Economics and management of American shipbuilding and the potential for commercial competitiveness. *Journal of Ship Production*, Vol. 12 (1), pp. 1-10.

5. Daidola, J. C., Parente, J., and W. H. Robinson. 1996. Producibility of double hull tankers. *Journal of Ship Production*, 12(1): 20–38.

6. ANSI/AWS D1.1-96, *Structural Welding Code — Steel*, American Welding Society, Miami, Fla.

7. AWS/AASHTO D1.5-95, *Bridge Welding Code*, American Welding Society.

8. Parrot, R. S., Ward, S. W., and Uttrachi, G. D. 1974. Electroslag welding speeds shipbuilding. *Welding Journal*, 53(4): 218–222.

9. Howser, B. C. 1985. Applications and trends in electroslag welding in the United States. *Proceedings of Electroslag Processing for Marine Applications*, Report EW-20-85, United States Naval Academy, pp. 4.1–4.11.

10. Yu, D. W., Ann H. S., Devletian, J. H., and Wood, W. E. 1986. Solidification study of narrow gap electroslag welds. *Welding Research: The State of the Art*, E. F. Nippes and D. J. Ball (eds.), ASM International, Materials Park, Ohio, pp. 21–32.

11. Yu, D. W., Ann, H. S., Devletian, J. H., and Wood, W. E. 1987. Improvements in microstructure and properties of steel electroslag weldments using low alloy tubular filler metal. *Welding Metallurgy of Structural Steels*, J. Y. Koo (ed.), The Metallurgical Society of AIME, Warrendale, Pa., pp. 233–254.

12. Wood, W. E., and Devletian, J. H. 1987. Improved Fracture Toughness and Fatigue Characteristics of Electroslag Welds, Publication No. FHWA/RD87/026, U.S. Department of Transportation Federal Highway Administration, Turner-Fairbank Highway Research Center, McLean, Va., p. 244.

13. Turpin, R. B., Scholl, M., Devletian, J., and Wood, W. 1983. Field welding of rail by the electroslag process. *Proceedings of Second International Heavy Haul Conference*, Colorado Springs, Colo., Paper-82-HH-16, pp. 142–157.

14. Juers, R. H., and McConnell, F. 1996. Electrogas welding of advanced double-hull subassemblies. *Welding Journal*, 75(1): 45–53.